Effect of Indium Content on the Melting Point, Dross, and Oxidation Characteristics of Sn-2Ag-3Bi-xIn Solders

Ae-Jeong Jeon
National Core Research Center (NCRC),
Pusan National University,
Pusan 609-735, Korea

Seong-Jun Kim
Samsung Electronics Co., Ltd.,
Suwon 443-742, Korea

Sang-Hoon Lee
Korea Institute of Materials Science,
Changwon 642-831, Korea

Chung-Yun Kang[1]
National Core Research Center (NCRC),
Pusan National University,
Pusan 609-735, Korea
e-mail: kangcy@pusan.ac.kr

This paper presents the effect of indium (In) content on the melting temperature, wettability, dross formation, and oxidation characteristics of the Sn-2Ag-3Bi-xIn alloy. The melting temperature of the Sn-2Ag-3Bi-xIn alloy ($2 \le x \le 6$) was lower than 473 K. The melting range between the solidus and liquidus temperatures was approximately 20 K, irrespective of the indium content. As the indium content increased, the wetting time increased slightly and the maximum wetting force remained to be mostly constant. The dross formation decreased to approximately 50% when adding 1In to Sn-2Ag-3Bi, and no dross formation was observed in the case of Sn-2Ag-3Bi-xIn alloy ($x \ge 1.5$) at 523 K for 180 min. Upon approaching the inside of the oxidized solder of the Sn-2Ag-3Bi-1.5In alloy from the surface, the O and In contents decreased and the Sn content increased based on depth profiling analysis using Auger electron spectroscopy (AES). The mechanism for restraining dross (Sn oxidation) of Sn-2Ag-3Bi alloy with addition of indium may be due to surface segregation of indium. This is due to the lower formation energy of indium oxide than those of Sn oxidation. [DOI: 10.1115/1.4023529]

Keywords: Sn-Ag-Bi-In alloy, wettability, dross, oxidation

1 Introduction

It is important to use unhazardous elements while developing lead-free solder alloys for electronics packaging. Further, the alloy should be designed such that its melting temperature is as low as that of the Sn-37Pb solder (456 K). Except for the melting temperature, there are many properties needed for the solder development such as wettability, dross formation, flux compatibility, mechanical properties, and thermal/electrical conductivities [1]. A low-temperature solder is required for minimizing heat damage and warpage during the process and for increasing the package density, e.g., for packaging on both sides of a printed circuit board (PCB). Numerous studies have been conducted on alloys based on Sn-Bi [2], Sn-Zn [3–7], and Sn-Ag [8–11]. The most widely used solder in electronics packaging is the Sn-3Ag-0.5Cu solder [12,13]. However, its melting temperature is approximately 34 K higher than that of the Sn-37Pb solder and it is not suitable for manufacturing mobile products because of its low drop shock reliability [14,15].

A number of studies on the characteristics of the Sn-Ag-Bi alloy have been conducted in the recent years [16–20]. The National Institute of Standards and Technology (NIST) in U.S. and Kattner and Boettinger presented the ternary phase diagram for Sn-Ag-Bi system and reported that the addition of bismuth (Bi) to the Sn-Ag alloy decreased the solidus and liquidus temperatures simultaneously [20,21]. However, the addition of Bi induces the lift-off phenomenon [18]. Therefore, a solder alloy with a low content of Bi, such as Sn-3Ag-(2-3)Bi and Sn-3.4Ag-4.8Bi, was developed. Further, in order to decrease the melting temperature and improve the drop shock reliability, indium was added to the Su-Ag [8,22,23], Sn-Ag-Bi, Sn-Ag-Cu [24] system to form customized alloys such as Sn-3.5Ag-3Bi-In, Sn-3Ag-2.5Bi-2.5In and Sn-2.5Ag-3Bi-1In-0.2Cu. In particular, the melting temperature of the Sn-Ag-Bi-In alloys is as low as 458–488 K, which is relatively lower than those of the Sn-Ag and Sn-Cu alloys and relatively close to that of the Sn-Pb alloy. However, to the best of the authors' knowledge, a very limited number of studies have been conducted on the effects of indium on the Sn-Ag-Bi system [25]. In this study, the effect of indium content on the melting temperature, wettability, dross formation, and oxidation of the Sn-2 wt. %Ag-3 wt. %Bi (i.e., Sn-2Ag-3Bi) system is investigated. The characteristics of the Sn-37Pb solder was compared with those of the Sn-Ag-Bi-In solder in order to assess its possible applications in preparing electronics packaging.

2 Experimental Procedure

The materials used in the experiment were melted in Ar atmosphere in an electric furnace, followed by casting to a diameter of 15 mm and length of 110 mm in a Cu mold. Differential scanning calorimetry (DSC) was used to investigate the melting temperature and melting range of the specimen. The specimen was subjected to a peak temperature of 573 K in air and then cooled to room temperature at a cooling rate of 10 K/min. The melting temperature was determined by taking the average of the values obtained from three tests conducted on each alloy composition.

The wettability test was conducted by using the meniscus method of the globule type. The time to buoyancy corrected zero value (zero cross time) and the maximum wetting force were measured as a function of the indium content, i.e., Sn-2Ag-3Bi-6In, Sn-2Ag-3Bi-4In, Sn-2Ag-3Bi-2In, and Sn-2Ag-3Bi. The wetting specimen had a weight of 200 mg, immersion depth of 0.3 mm, immersion time of 5 s, soldering temperature of 528 K, and flux with RH-15SH-RMA type. The wetting time and force were determined by taking the average of the values obtained from 15 tests conducted for each alloy. Figure 1 presents the typical wetting curve from the meniscus method.

The oxidation test was conducted as follows. First, a 50-g specimen was inserted into a stainless steel pot and melted at 523 K on a hot plate. Next, the melt was stirred with a ceramic rod at 100 rpm. The dross oxidation amount was measured every

[1]Corresponding author.

Contributed by the Electronic and Photonic Packaging Division of ASME for publication in the Journal of Electronic Packaging. Manuscript received September 4, 2012; final manuscript received January 4, 2013; published online March 28, 2013. Assoc. Editor: S. B. Park.

 Copyright © 2013 by ASME

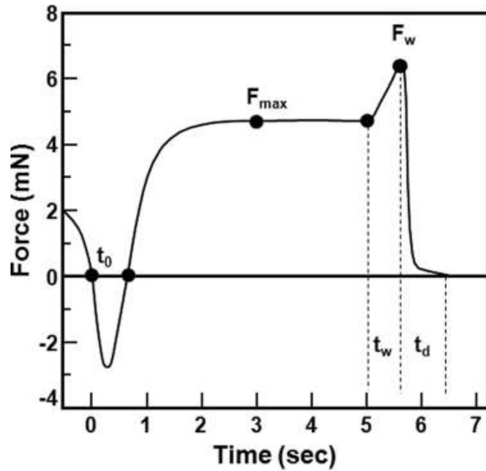

Fig. 1 A typical wetting curve from meniscus method; t_0 = start point to wet; t_w = peak time; t_d = drop time; F_{max} = maximum wetting force; and F_w = maximum withdrawal force

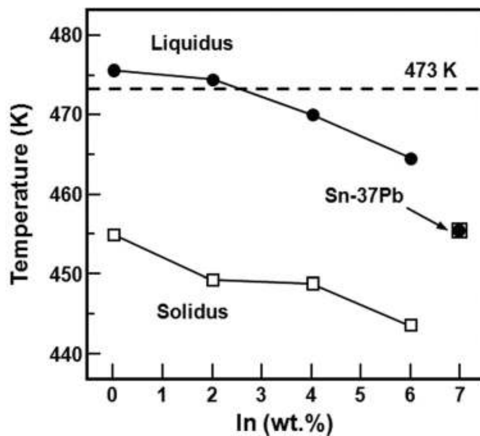

Fig. 2 Melting temperature for Sn-2Ag-3Bi-xIn as a function of indium content

30–180 min. The oxidation product consisted of pure oxides as well as the solder metal. Therefore, it was necessary to separate the pure oxidation product from the sludge by using a 710-μm mesh. Finally, the weight of the dross was measured only from the pure oxide.

The microstructure of the specimen was observed by optical microscopy (OM) and scanning electron microscopy (SEM). A mixture of ethyl alcohol (95 ml), HNO_3 (4 ml), and HCl (1 ml) was used as the etching solution. Phase identification was performed by X-ray diffraction (XRD) analysis. Depth profiling using the surface analytical technique of Auger electron spectroscopy (AES) was employed for determining the composition variation from the oxidized surface layer to the inside of the specimen.

3 Results and Discussion

3.1 Melting Temperature and Wettability. Figure 2 shows the liquidus and solidus temperatures for Sn-2Ag-3Bi-xIn, where x varies from 0 to 6 wt. %. As the indium content increased, the liquidus and solidus temperatures decreased simultaneously. The melting range between the liquidus and solidus temperatures was approximately 20 K, irrespective of the indium content.

For 2 wt. %In, the liquidus temperature was 475 K, i.e., 2 K higher than 473 K. As the indium content increased to 4 wt. % and 6 wt. %, the liquidus temperature decreased below 473 K and was

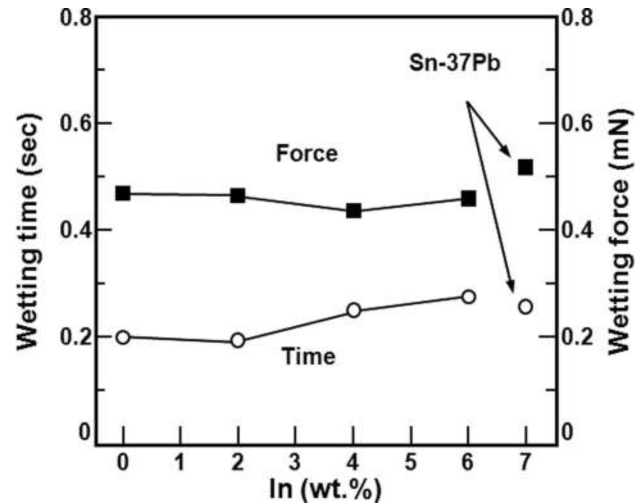

Fig. 3 Wetting time and maximum wetting force with respect to the indium content

slightly higher (10–15 K) than the melting temperature of the Sn-37Pb solder (456 K). The development of lead-free solders whose melting temperatures are lower than 473 K is very important because the existing soldering process and equipment for the Sn-Pb solder can be used continuously. Therefore, the Sn-2Ag-3Bi-xIn ($2 \leq x \leq 6$) alloy is compatible with the soldering process with respect to its melting temperature.

Wettability is known to be good as force is bigger and time is shorter. Figure 3 indicates the wetting time (t_0) and the maximum wetting force (F_{max}) for the Sn-2Ag-3Bi-xIn ($0 \leq x \leq 6$) alloy. As the indium content increased, t_0 increased; however, F_{max} remained mostly constant. In comparison to the Sn-37Pb alloy, F_{max} for the Sn-2Ag-3Bi-xIn was slightly lower, while t_0 was mostly constant. Therefore, the Sn-2Ag-3Bi-xIn ($2 \leq x \leq 6$) alloy is compatible with the soldering process with respect to its wettability, although its wettability decreases with an increase in the indium content.

3.2 Dross Characteristics. The surface morphology and cross section of the dross produced from the Sn-2Ag-3Bi solder are shown in Fig. 4. The dross was in the shape of sponge powder, and it consisted of the solder alloy on the inside and oxides on the surface, as shown in Fig. 4(*b*). Figure 5 shows the result of the XRD analysis of the dross. The solder alloy on the inside was Sn and the surface oxide was SnO. The dross produced from the Sn-2Ag-3Bi, Sn-2Ag-3Bi-1In, Sn-2Ag-3Bi-1.5In, and Sn-37Pb solders comprised tin oxides in which SnO was dominant over SnO_2.

Figure 6 indicates the total amount of dross as a function of the holding time in the dross test. The change in dross weight with holding time for the Sn-2Ag-3Bi and the Sn-37Pb solders was almost similar. However, the dross weight for the Sn-2Ag-3Bi-1In solder decreased to approximately 50%. Finally, after a holding time of 3 h, there was no dross formation when the indium content increased to 1.5 wt. % in the Sn-2Ag-3Bi solder. When the indium content increased to 2–6 wt. % in the Sn-2Ag-3Bi solder, no further dross formation was observed during the dross test. The relationship between dross weight and holding time was rearranged to the square of dross weight versus the holding time, as indicated in Fig. 7. The square of the dross weight had a linear relationship with the holding time, i.e., the dross formation rate had a parabolic nature to the holding time. The dross formation rate in such cases is normally dependent on the kinetics of the diffusion-controlled reaction, which is specifically associated with the composition of the oxide layer and its thickness. Therefore, the dross formation rate for the Sn-Ag-Bi solders depended on the oxidation rate of Sn. However, Figs. 6 and 7 show that the addition of indium to

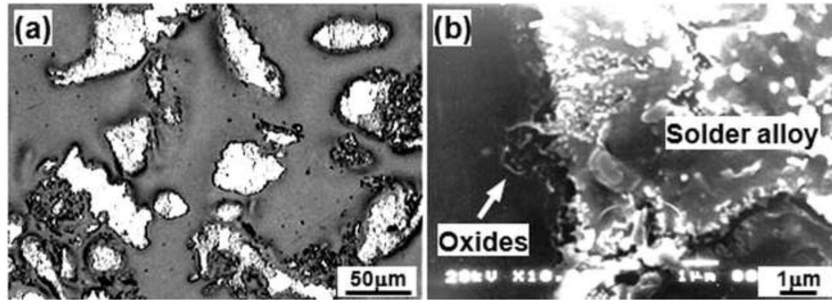

Fig. 4 Shape of the dross in Sn-2Ag-3Bi alloy stored at 523 K for 30 min; (*a*) surface morphology (OM) and (*b*) cross section (SEM)

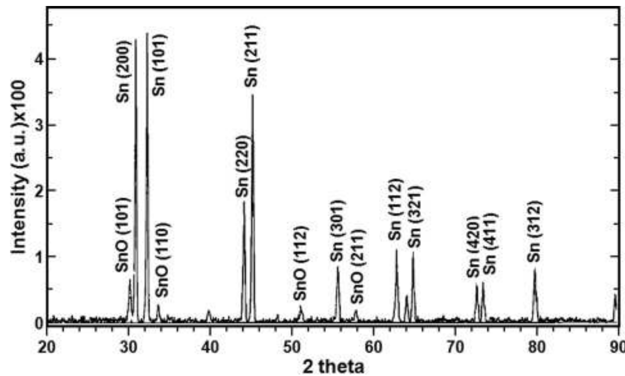

Fig. 5 XRD analysis on the dross produced in Sn-2Ag-3Bi alloy stored at 523 K for 30 min

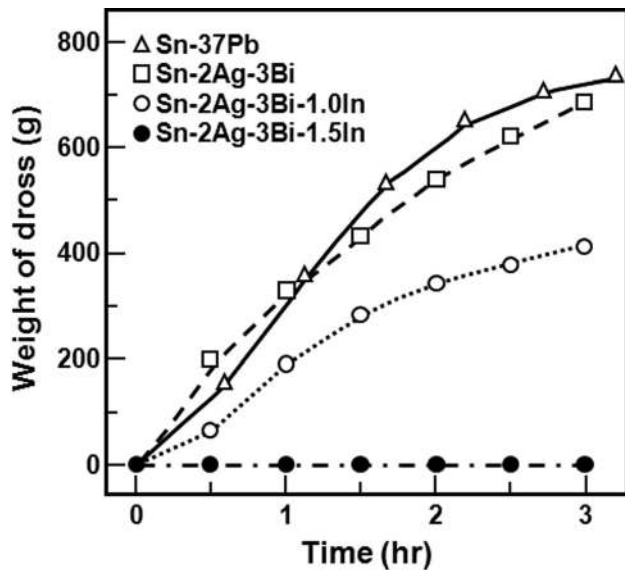

Fig. 6 Dross weight versus holding time for Sn-2Ag-3Bi-xIn and Sn-37Pb solders

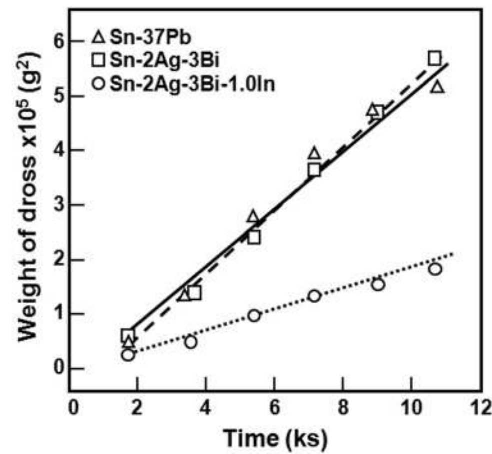

Fig. 7 Square of dross weight versus holding time for Sn-2Ag-3Bi-xIn and Sn-37Pb solders

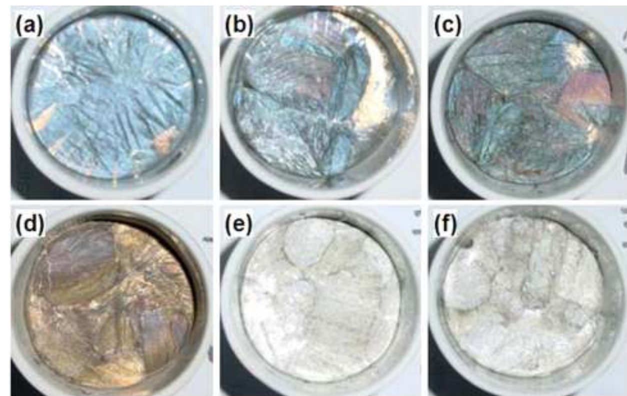

Fig. 8 Oxidized surface for the solders stored at 523K for 1 h. (*a*) Sn-37Pb, (*b*) Sn-2Ag, (*c*) Sn-2Ag-3Bi, (*d*) pure indium, (*e*) Sn-2Ag-3Bi-1In, and (*f*) Sn-2Ag-3Bi-1.5In.

the Sn-2Ag-3Bi alloy restrained the oxidation of the solder alloy and decreased the dross formation rate. When the amount of indium added to the Sn-2Ag-3Bi alloy was increased beyond 1.5 wt. %, there was no dross formation.

3.3 Oxidation Characteristics at High Temperatures. In order to understand the restraint of oxidation induced by the addition of indium, the oxidation behavior was observed as a function of the indium content during high-temperature storage. The solders were heated to 523 K for 1 h in air. Figure 8 shows the color variation of the solder surface as a function of the alloying elements.

The color of the Sn-2Ag-3Bi alloy was dark blue, which is the same as that of pure Sn. The colors of the pure In and the Sn alloy which does not include indium element were gold and blue, respectively. However, the colors of both the Sn-2Ag-3Bi-1In and Sn-2Ag-3Bi-1.5In alloys were light gray or silver. By comparing the color variation of the alloys, it was found that the Sn-2Ag-3Bi and Sn-37Pb alloys were tarnished mainly because of Sn oxidation, since they produced the same color (dark blue) with pure Sn. By adding indium to the Sn-2Ag-3Bi alloy, Sn oxidation was restrained and the other mechanisms, e.g., indium oxidation, were probably controlled for the oxidation.

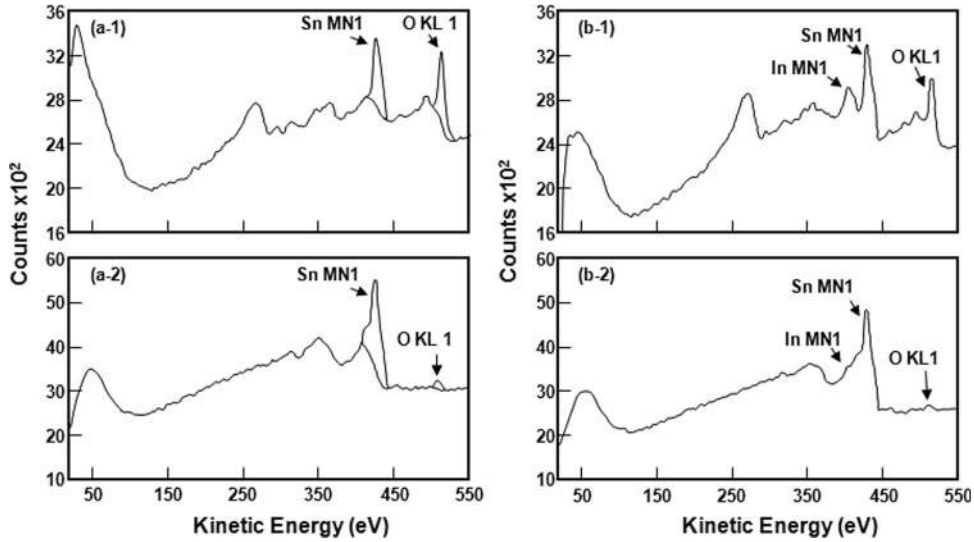

Fig. 9 AES analysis for the oxidized surface; (*a*) Sn-2Ag-3Bi, (*b*) Sn-2Ag-3Bi-1.5In, and (1) surface, (2) inside

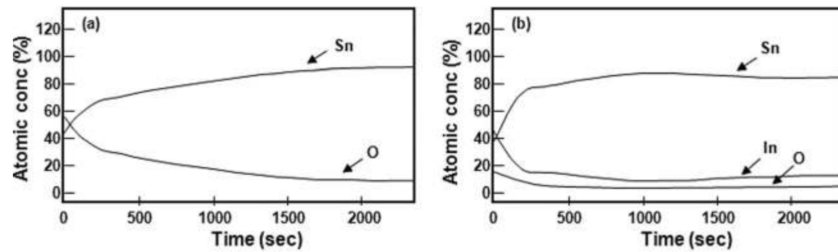

Fig. 10 Concentration distribution from the surface to the inside of the oxidized solder; (*a*) Sn-2Ag-3Bi and (*b*) Sn-2Ag-3Bi-1.5In

Figure 9 indicates the results of the element analysis of the oxidized surface for two specimens, i.e., the Sn-2Ag-3Bi alloy and the Sn-2Ag-3Bi-1.5In alloy. Depth profiling using AES was conducted for 2370 s in order to measure the concentration variation of each element in the depth direction. The concentration profiles of the in situ depth analysis are shown in Fig. 10. The oxidized surface for the Sn-2Ag-3Bi alloy had the Sn and O peaks (Fig. 9(*a*-1)). Upon approaching the solder inside the alloy, the Sn concentration increased and the O concentration decreased (Figs. 9(*a*-2) and 10(*a*)). The oxidized surface of the Sn-2Ag-3Bi-1.5In alloy showed Sn, O, and In peaks (Fig. 9(*b*-1)). Upon approaching the inside of the oxidized solder from the surface, the Sn content increased and the O/In contents decreased (Figs. 9(*b*-2) and 10(*b*)). In Fig. 10(*b*), it is shown that the surface has much higher Indium concentration than the bulk(1.5 wt. %(1.6 at. %)In). It is almost 40 at. % at the surface, and diminishes to a few or several percent as it is sputtered to depth. Thus, the mechanism for slowing down oxidation of Sn-2Ag-3Bi alloy with addition of indium may be due to surface segregation of indium. Figure 11 presents the change of free energy for formation of oxide of Sn, Ag, Bi and In Ref. [26]. The oxide formation energy of In was lower than those of Sn. This means that the indium oxide layer was previously produced on the surface at the beginning of oxidation. From these results, it is clear that formation of the indium oxide on the surface in the Sn-2Ag-3Bi-In solder was protected against Sn oxidation formation, i.e., dross formation.

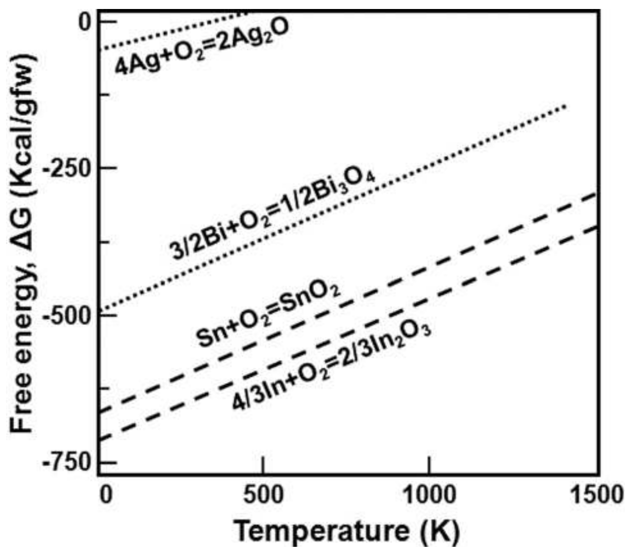

Fig. 11 Standard Gibbs energies of formation for oxide [26]

4 Conclusions

The effect of indium content on the melting temperature, wettabililty, dross formation, and oxidation characteristics of the Sn-2Ag-3Bi-xIn alloy was investigated.

(1) The liquidus temperature decreased from 477 K to 465 K as the indium content increased from 0 to 6 wt. %. The melting range between the solidus and liquidus temperatures

was approximately 20 K, irrespective of the indium content. The melting temperature of the Sn-2Ag-3Bi-xIn alloy ($2 \leq x \leq 6$) was lower than the objective (473 K).

(2) For the Sn-2Ag-3Bi-xIn ($2 \leq x \leq 6$) alloy, the wetting time (t_0) increased slightly and the maximum wetting force (F_{max}) was mostly constant. The wettability of the Sn-2Ag-3Bi-xIn ($2 \leq x \leq 6$) alloy was compatible with the Sn-37Pb alloy.

(3) The change of dross weight with holding time for the Sn-2Ag-3Bi and the Sn-37Pb solders was almost similar, while the dross weight for the Sn-2Ag-3Bi-1In solder decreased to approximately 50%. There was no dross formation when the indium content increased to more than 1.5 wt. % in the Sn-2Ag-3Bi solder.

(4) The mechanism for slowing down oxidation of Sn-2Ag-3Bi alloy with addition of indium may be due to surface segregation of indium. Because the oxide formation energy of In was lower than those of Sn, the indium oxide layer was previously produced on the surface at the beginning of oxidation. It is clear that the formation of the indium oxide on the surface in the Sn-2Ag-3Bi-In solder was protected against dross formation.

Acknowledgment

This work was supported by the National Research Foundation of Korea (NRF) Grant funded by the Ministry of Education, Science and Technology (NRF-2012R1A5A1048294).

References

[1] Wood, E. P., and Nimmo, K. L., 1994, "In Search of New Lead-Free Electronic Solders," J. Electron. Mater. **23**, pp. 709–713.
[2] Miao, H.-W., Duh, J.-G., 2001, "Microstructural Evolution in Sn-Bi and Sn-Bi-Cu Solder Joints Under Thermal Aging," Mater. Chem. Phys., **71**, pp. 255–271.
[3] Islam, M. N., Chan, Y. C., Rizvi, M. J., and Jillek, W., 2005, "Investigations of Interfacial Reactions of Sn-Zn Based and Sn-Ag-Cu Lead-Free Solder Alloys as Replacement for Sn-Pb Solder," J. Alloys Compd., **400**, pp. 136–144.
[4] Zhou, J., Sun, Y., Xue, F., 2005, "Properties of Low Melting Point Sn–Zn–Bi Solders," J. Alloys Compd., **397**, pp. 260–264.
[5] Duan, L. L., Yu, D. Q., Han, S. Q., Ma, H. T., and Wang, L., 2004, "Microstructural Evolution of Sn–9Zn–3Bi Solder/Cu Joint During Long-Term Aging at 170 °C," J. Alloys Compd., **381**, pp. 202–207.
[6] Garcia, L. R., Osório, W. R., Peixoto, L. C., and Garcia, A., 2010, "Mechanical Properties of Sn–Zn Lead-Free Solder Alloys Based on the Microstructure Array," Mater. Charact., **61**, pp. 212–220.
[7] Kim, K. S., Yang, J. M., and Yu, C. H., 2003, "Microstructures and Shear Strength of Sn-Zn Lead-Free Solder Joints," J. Korean Weld. Soc., **21**, pp. 765–770.
[8] Huang, M. L., and Wang, L., 2005, "Effects of Cu, Bi, and In on Microstructure and Tensile Properties of Sn-Ag-X(Cu, Bi, In) Solders," Metall. Mater. Trans. A, **36**, pp. 1439–1446.
[9] Kang, S. K., Choi, W. K., Shih, D. Y., Henderson, D. W., Gosselin, T., Sarkhel, A., Goldsmith, C., and Puttlitz, K. J., 2003, "Study of Ag_3Sn Plate Formation in the Solidification of Near Ternary Eutectic Sn-Ag-Cu Alloys," JOM, **55**, pp. 61–65.
[10] Kim, K. S., Huh, S. H., and Suganuma, K., 2003, "Effects of Fourth Alloying Additive on Microstructures and Tensile Properties of Sn–Ag–Cu Alloy and Joints With Cu," Microelectron. Reliab., **43**, pp. 259–267.
[11] Fawzy, A., 2007, "Effect of Zn Addition, Strain Rate and Deformation Temperature on the Tensile Properties of Sn–3.3 wt.% Ag Solder Alloy," Mater. Charact., **58**, pp. 323–331.
[12] Bradley, E., Handwerker, C., and Sohn, J. E., 2003, "NEMI Report: A Single Lead-Free Alloy is Recommended," SMT, pp. 24–25.
[13] Hong, W. S., Kim, W. S., Park, N. C., and Kim, K. B., 2007, "Activation Energy for Intermetallic Compound Formation of Sn-40Pb/Cu and Sn-3.0Ag-0.5Cu/Cu Solder Joints," J. Korean Weld. Joining Soc., **25**, pp. 184–190.
[14] Amagai, M., Toyoda, Y., and Tajima, T., 2003, "High Solder Joint Reliability With Lead Free Solders," Proceedings of IEEE 53rd Electronic Component Technology Conference, New Orleans, May 27–30, pp. 317–322.
[15] Lee, J. E., Kim, K. S., and Huh, S. H., 2011, "Development of Sn-Zn Based Low Temperature Lead-Free Solder for Improvement of Oxidation Resistance," J. Korean Weld. Joining Soc. **29**, pp. 514–521.
[16] Kim, K. S., Imanishi, T., Suganuma, K., Ueshima, M., and Kato, R., 2007, "Properties of Low Temperature Sn-Ag-Bi-In Solder Systems," Microelectron. Reliab., **47**, pp. 1113–1119.
[17] Song, J. M., Wu, Z. M., and Huang, D. A., 2007, "Two Stage Nonequilibrium Eutectic Transformation in a Sn-3.5Ag-3In Solder," Scr. Mater., **56**, pp. 413–416.
[18] Yeh, M. S., 2003, "Effects of Indium on the Mechanical Properties of Ternary Sn-In-Ag Solders," Metall. Mater. Trans. A, **34**, pp. 361–365.
[19] Abd El-Salam, F., Abd El-Khalek, A. M., Nada, R. H., and Fawzy, A., 2008, "Effect of Silver Addition on the Creep Parameters of Sn–7 wt.% Bi Alloy During Transformation," Mater. Charact., **59**, pp. 9–17.
[20] Kattner, U. R., and Boettinger, W. J., 1994, "On the Sn-Bi-Ag Ternary Phase Diagram," J. Electron. Mater., **23**(7), pp. 603–610.
[21] Metallurgy Division, National Institute of Standards and Technology (NIST) of U.S. Commerce Department.
[22] Amagai, M., Toyoda, Y., Ohnishi, T., and Akita, S., 2004, "High Drop Test Reliability: Lead-Free Solders," Proceedings of IEEE 54th Electronic Component Technology Conference, Las Vegas, June 1–4, pp. 1304–1309.
[23] McComack, M., and Jin, S. H., 1993, "Progress in the Design of New Lead-Free Solder Alloys," JOM, **45**, pp. 36–40.
[24] Takemoto, T., 2000, "The Recent Situation of Lead-Containing Solder Regulation and Replacement to Environmentally Compatible Lead-Free Solder," J. Weld. Soc., **69**, pp. 100–107.
[25] Glazer, J., 1994, "Microstructure and Mechanical Properties of Lead Free Alloys for Low Cost Electronic Assembly—A Review," J. Electron. Mater., **23**, pp. 693–700.
[26] Howard, S. M., 2006, "Ellingham Diagrams: Standard Gibbs Energies of Formation for Oxides," SD School of Mines and Technology, Rapid City, SD.